Journal of Zhejiang University-SCIENCE A (Applied Physics & Engineering)
ISSN 1673-565X (Print); ISSN 1862-1775 (Online)
www.zju.edu.cn/jzus; www.springerlink.com
E-mail: jzus@zju.edu.cn

Lumped parameter model for resonant frequency estimation of a thermoacoustic engine with gas-liquid coupling oscillation*

Ke TANG†, Tian LEI, Xiao-gang LIN, Tao JIN†‡, Yu ZHANG

(*Institute of Refrigeration and Cryogenics, Zhejiang University, Hangzhou 310027, China*)

†E-mail: ktang@zju.edu.cn; jintao@zju.edu.cn

Received Apr. 21, 2010; Revision accepted Sept. 21, 2010; Crosschecked Jan. 25, 2011

Abstract: Gas-liquid coupling oscillation is a novel approach to reducing the resonant frequency and to elevating the pressure amplitude of a thermoacoustic engine. If a thermoacoustic engine is used to drive low-frequency pulse tube refrigerators, the frequency matching between the thermoacoustic engine and the refrigerator plays an important role. Based on an acoustic-electric analogy, a lumped parameter model is proposed to estimate the resonant frequency of a standing-wave thermoacoustic engine with gas-liquid coupling oscillation. Furthermore, a simplified lumped parameter model is also developed to reduce the computation complexity. The resonant frequency dependence on the mean pressure, the gas space volume, and the water column length is computed and analyzed. The impact of different working gases on the resonant frequency is also discussed. The effectiveness of the models is validated by comparing the computed results with the experimental data of the gas-liquid coupling oscillation system. An increase in the mean working pressure can lead to a rise in the resonant frequency, and a lower resonant frequency can be achieved by elongating the liquid column. In comparison with nitrogen and argon, carbon dioxide can realize a lower frequency due to a smaller specific heat ratio.

Key words: Thermoacoustic engine, Gas-liquid coupling oscillation, Acoustic-electric analogy, Resonant frequency
doi:10.1631/jzus.A1000191 **Document code:** A **CLC number:** TB51+1

1 Introduction

The thermoacoustic engine, without any moving components, has attracted much interest in recent years, especially in the potential applications of refrigeration and electricity generation (Backhaus *et al.*, 2004; Chen *et al.*, 2004; Castrejón-Pita and Huelsz, 2007). In order to improve the performance of a thermoacoustically driven pulse tube refrigerator, much effort has been made to lower the resonant frequency and to elevate the pressure amplitude of thermoacoustic engines (Sugita *et al.*, 2004; Dai *et al.*, 2005; Tang *et al.*, 2005; 2007; 2008; Hu *et al.*, 2007; Yu *et al.*, 2007). Gas-liquid coupling oscillation is a novel approach for reducing the resonant frequency and for elevating the pressure amplitude of a thermoacoustic engine. Compared with the system merely using nitrogen gas (N_2), introduction of a water column of 1.5 kg resulted in a drop of resonant frequency by 79.0% and a rise of pressure amplitude by 157.4% (Tang *et al.*, 2009). Castrejón-Pita and Huelsz (2007) reported a heat-to-electricity thermoacoustic-magnetohydrodynamic conversion system with air and aqueous solution as working fluids, which demonstrated the feasibility of electricity generation by a thermoacoustic engine with gas-liquid coupling oscillation. Earlier studies on gas-liquid coupling oscillation systems were mainly focused on the liquid piston Stirling engines aimed at pumping water (West, 1983).

The frequency matching between the engine and the refrigerator is of great importance for a

‡ Corresponding author

* Project supported by the National Natural Science Foundation of China (No. 50806065), and the Research Fund for the Doctoral Program of Higher Education of China (No. 200803351053)

thermoacoustically driven pulse tube refrigeration system. The resonant frequency of thermoacoustic engines has been widely studied, typically by the network model method (Chen *et al.*, 2002; Tu *et al.*, 2003; Dai *et al.*, 2006). However, the resonant frequency estimations in reported works were all conducted for the thermoacoustic engines with gas oscillation.

This paper focuses on the resonant frequency of a thermoacoustic engine with gas-liquid coupling oscillation. Based on an acoustic-electric analogy, a lumped parameter model is proposed to analyze the resonant frequency of a standing-wave thermoacoustic engine with gas-liquid coupling oscillation. The acoustic-electric analogy is considered as an intuitionistic approach to revealing the essence of working fluid resonance inside the thermoacoustic engine. With a resonant frequency below 10 Hz (Tang *et al.*, 2009), the wavelength (beyond 30 m for nitrogen) is much longer than the characteristic dimensions of the engine components. Thus, the lumped parameter model is reasonable for the resonant frequency computation. In addition, a simplified lumped parameter model is also developed to reduce computation complexity. The influences of the mean working pressure, the gas space volume, the water column length, and different working gases on the resonant frequency are computed and discussed with these two models. Experiments are also conducted to validate the effectiveness of the computation.

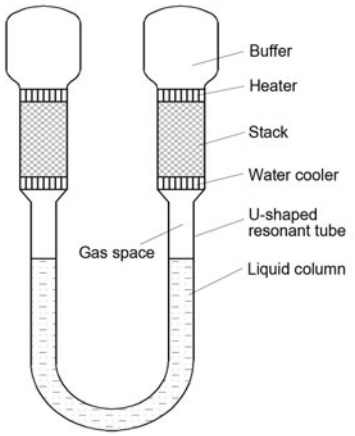

Fig. 1 Schematic of a standing-wave thermoacoustic engine with gas-liquid coupling oscillation

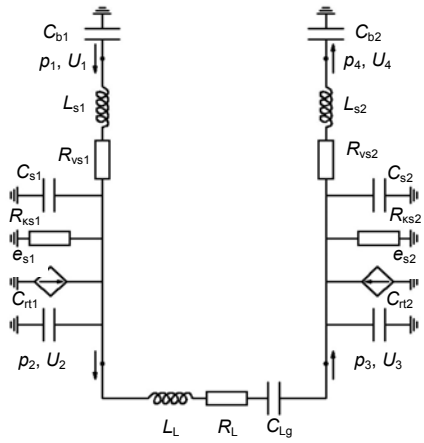

Fig. 2 Circuit of lumped parameter model (LPM) based on acoustic-electric analogy

2 Acoustic-electric analogy analysis

2.1 Lumped parameter model

A standing-wave thermoacoustic engine with gas-liquid coupling oscillation is schematically shown in Fig. 1. The engine employs a symmetrical configuration, consisting of two buffers, two heaters, two stacks, two water coolers, one U-shaped resonant tube, and one water column.

Based on the acoustic-electric analogy (Swift, 2002), the engine can be expressed as a circuit of lumped parameter model (LPM) (Fig. 2). The compliances C_b and C_{rt} stand for the buffer and the gas space above the liquid in a resonant tube, respectively. The inertance L_s and the resistance R_{vs} in series combined with the shunt-wound compliance C_s, resistance R_{KS}, and controlled source e_s represent the stack. The compliances C_b, C_{rt}, and C_s derive from the compressibility of working gas, while the inertance L_s reflects the mass inertia. The resistances R_{vs} and R_{KS} result from the viscosity and the thermal relaxation effect, respectively. The coefficient of controlled source e_s expresses the volume flow rate amplification effect due to the thermal-acoustic conversion. The subscripts 1 and 2 represent the left and right branches. Based on the symmetric configuration, C_{b1} equals to C_{b2}, while L_s, R_{vs}, C_s, R_{KS}, and C_{rt} have similar expressions. However, e_{s1} equals to $-e_{s2}$ due to the opposition of temperature gradients along the left and right stacks. The detailed formulas for the above parameters have been described in (Swift, 2002).

The heater and the water cooler are considered to be a section of the stack in the acoustic-electric analogy model, since their flow channels are short and similar to that of the stack.

Further attention is paid to the acoustic-electric analogy of the liquid column. The momentum equation of the liquid column is

$$\rho_{\mathrm{L}} A_{\mathrm{L}} l_{\mathrm{L}} \frac{\mathrm{d}^2 h_{\mathrm{L}}}{\mathrm{d}t^2} = A_{\mathrm{L}} \Delta p - 2A_{\mathrm{L}} \rho_{\mathrm{L}} g h_{\mathrm{L}} - f_{\mathrm{f}} \frac{\mathrm{d}h_{\mathrm{L}}}{\mathrm{d}t}, \quad (1)$$

where ρ_{L}, A_{L}, l_{L}, and h_{L} are the density, section area, length, and distance apart from the equilibrium position of the liquid column, respectively; Δp, g, f_{f}, and t are pressure difference between two ends of the liquid column, gravitational acceleration, friction factor, and time, respectively.

Substitution of the volume flow rate $U = A_{\mathrm{L}} \frac{\mathrm{d}h_{\mathrm{L}}}{\mathrm{d}t}$ into Eq. (1) gives

$$\frac{\rho_{\mathrm{L}} l_{\mathrm{L}}}{A_{\mathrm{L}}} \frac{\mathrm{d}U}{\mathrm{d}t} + \frac{2\rho_{\mathrm{L}} g}{A_{\mathrm{L}}} \int U \mathrm{d}t + \frac{f_{\mathrm{f}}}{A_{\mathrm{L}}^2} U = \Delta p. \quad (2)$$

According to Eq. (2), the liquid column can be analogized as a combination of an inertance L_{L}, a compliance C_{Lg}, and a resistance R_{L} in series:

$$L_{\mathrm{L}} = \rho_{\mathrm{L}} l_{\mathrm{L}} / A_{\mathrm{L}}, \quad (3)$$

$$C_{\mathrm{Lg}} = A_{\mathrm{L}} / (2\rho_{\mathrm{L}} g), \quad (4)$$

$$R_{\mathrm{L}} = f_{\mathrm{f}} A_{\mathrm{L}}^2. \quad (5)$$

Note that the compliance C_{Lg} is not attributed to the compressibility of liquid (usually incompressible) as the above gas compliances of C_{b}, C_{rt}, and C_{s}, but to the gravity of the liquid column. As a result, C_{Lg} is series-wound with L_{L} and R_{L}, while C_{b}, C_{rt}, and C_{s} are all connected to the ground in parallel (Fig. 2). The subscript g indicates the effect of gravity.

For the circuit shown in Fig. 2, we have

$$U_1 = -\mathrm{i}\omega C_{\mathrm{b}} p_1, \quad (6)$$

$$p_2 = p_1 - U_1 (\mathrm{i}\omega L_{\mathrm{s}} + R_{\mathrm{vs}}), \quad (7)$$

$$U_2 = U_1 - \frac{p_2}{1/(\mathrm{i}\omega C_{\mathrm{s}}) + R_{\mathrm{ks}} + 1/(\mathrm{i}\omega C_{\mathrm{rt}})} + e_{\mathrm{s}} U_1, \quad (8)$$

$$p_3 = p_2 - U_2 (\mathrm{i}\omega L_{\mathrm{L}} + R_{\mathrm{L}} + 1/(\mathrm{i}\omega C_{\mathrm{Lg}})), \quad (9)$$

$$U_3 = U_2, \quad (10)$$

$$p_4 = p_3 - U_4 (\mathrm{i}\omega L_{\mathrm{s}} + R_{\mathrm{vs}}), \quad (11)$$

$$U_4 = \frac{U_3 - \dfrac{p_3}{1/(\mathrm{i}\omega C_{\mathrm{s}}) + R_{\mathrm{ks}} + 1/(\mathrm{i}\omega C_{\mathrm{rt}})}}{1 + e_{\mathrm{s}}}, \quad (12)$$

$$U_4 = \mathrm{i}\omega C_{\mathrm{b}} p_4, \quad (13)$$

where U is the volume flow rate amplitude, and p is the pressure amplitude. The solution of the simultaneous Eqs. (6) to (13), requiring iteration computation, gives the resonant angular frequency ω, and then the resonant frequency $f=\omega/2\pi$.

2.2 Simplified lumped parameter model

For the resonant characteristics which mainly depend on the inertance and the compliance, the circuit in Fig. 2 can be simplified by eliminating viscous resistance, thermal relaxation resistance, and controlled source of the volume flow rate, which helps to reduce the inconvenience of LPM due to iteration computation. The gas inertance in stack L_{s}, which is much smaller than that of liquid column L_{L}, is also omitted. The circuit of the simplified lumped parameter model (SLPM) is shown in Fig. 3. Considering the symmetric configuration, the resonant angular frequency from the SLPM is

$$\omega = \left(\frac{2}{L_{\mathrm{L}} (C_{\mathrm{b}} + C_{\mathrm{s}} + C_{\mathrm{rt}})} + \frac{1}{L_{\mathrm{L}} C_{\mathrm{Lg}}} \right)^{1/2}. \quad (14)$$

Substituting Eqs. (3) and (4) into Eq. (14), we have

$$\omega = \left(\frac{2A_{\mathrm{L}}}{\rho_{\mathrm{L}} l_{\mathrm{L}} (C_{\mathrm{b}} + C_{\mathrm{s}} + C_{\mathrm{rt}})} + \frac{2g}{l_{\mathrm{L}}} \right)^{1/2}. \quad (15)$$

The resonant angular frequency can be conveniently estimated with Eq. (15).

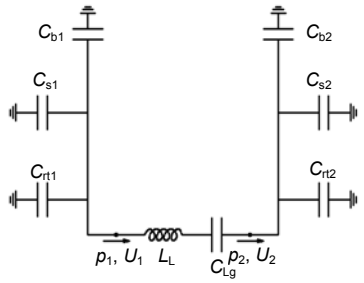

Fig. 3 Circuit of simplified lumped parameter model (SLPM) based on acoustic-electric analogy

3 Computed results and validation

The LPM and SLPM are both used to calculate the resonant frequency of the thermoacoustic engine, as shown in Fig. 1. The main dimensions of the engine are given in Table 1. The liquid column is water, and the working gas is N_2 except for the cases discussing the influence of working gases. The analysis mainly focuses on the impacts of the mean working pressure p_m, gas space volume V_{rt} (above the water level in the resonant tube), water column length l_L, and different working gases on resonant frequency.

Table 1 Dimensions of the standing-wave thermoacoustic engine

Component	Diameter (m)	Length (m)
Heater	0.056	0.064
Stack	0.056	0.285
Water cooler	0.056	0.034
U-shaped resonant tube	0.035	2.314
Hot buffer volume (L)	1.35	

As shown in Fig. 4, the results from the LPM and SLPM both indicate that the resonant frequency increases with an increase in the mean working pressure, which can be attributed to the effect of the mean working pressure on the compliance of working gas ($C=V/(\gamma p_m)$, where V, γ, and p_m are the volume, specific heat ratio, and mean working pressure, respectively). The inversely proportional function leads to a decrease in compliance C with an increase in mean working pressure p_m, and then the resonant frequency increases with the decreased compliance (Eq. (15)). The comparison of the computed results and experimental data indicates that both LPM and SLPM can give a reasonable estimation of the resonant frequency (Fig. 4).

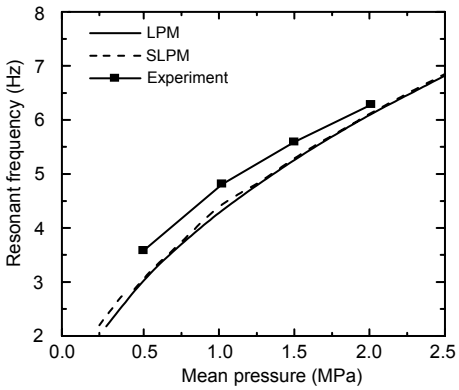

Fig. 4 Resonant frequency as a function of the mean working pressure p_m, with a gas space volume V_{rt} of 0.363 L and a water column length l_L of 1.56 m

The computed resonant frequency as a function of the gas space volume V_{rt} is shown in Fig. 5. In the computation, the variation of the gas space volume V_{rt} is realized by changing the resonant tube length. The compliance is proportional to the volume, and thus, the addition of gas space volume V_{rt} results in an increase in compliance C_{rt}. Consequently, the resonant frequency decreases with the addition of the gas space volume V_{rt} (Fig. 5).

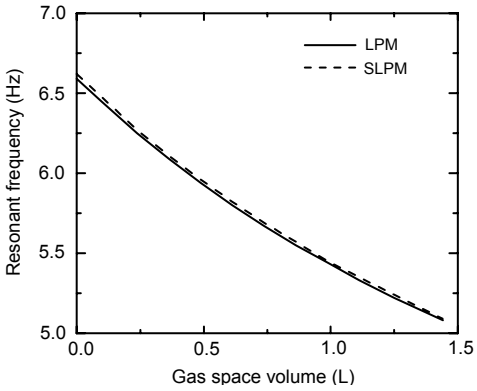

Fig. 5 Resonant frequency as a function of the gas space volume V_{rt}, with a mean working pressure p_m of 2.0 MPa and a water column length l_L of 1.56 m

The dependence of the resonant frequency on the water column length l_L is computed and shown in Fig. 6. The mean working pressure p_m is also set to 2.0 MPa, the gas space volume V_{rt} is 0.363 L, and the variation of water column length means a change of the resonant tube length. The inertance of the water column is proportional to its length (Eq. (3)), and the resonant frequency is inversely proportional to the square root of water column inertance (Eq. (14)). As a result, an addition of the water column length leads to a decrease in the resonant frequency.

In practice, for a given thermoacoustic engine apparatus, the dimensions of the resonant tube are fixed. An elongation of the water column will lead to a decrease in the gas space volume, and these two aspects pose opposite effects on the resonant frequency, according to Figs. 5 and 6. To study the collective impact of the water column length and the gas space volume, both computation and experiment have been performed with a resonant tube of 2.314 m in length.

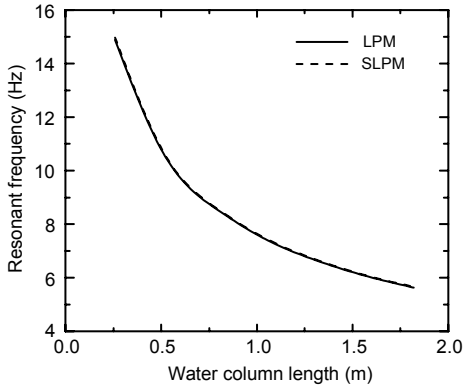

Fig. 6 Resonant frequency as a function of the water column length l_L, with a mean working pressure p_m of 2.0 MPa and a gas space volume V_{rt} of 0.363 L

The computed results and the experimental data, given in Fig. 7, indicate that the resonant frequency remarkably decreases with an elongation of the water column; i.e., water column length can be considered as the dominant factor (compared with the gas space volume). The computed curve in Fig. 7 shows the accordance with the experimental data, with an error less than 6%.

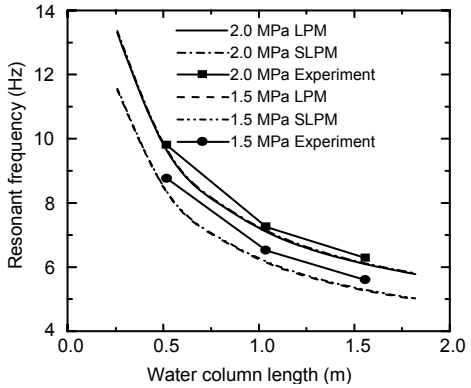

Fig. 7 Resonant frequency as a function of the water column length l_L, with the mean working pressures p_m of 2.0 MPa and 1.5 MPa and a resonant tube of 2.314 m in length

Additionally, the compliance of the working gas depends on the specific heat ratio. Thus, different working gases will also have an influence on the resonant frequency via their specific heat ratios. Table 2 shows the resonant frequency in the cases with argon (Ar), N_2, and CO_2 as working gases. The computed results with the two models and experimental data indicate that the argon-water system achieves the highest resonant frequency due to the argon's largest specific heat ratio, while the CO_2-water system achieves the lowest since the CO_2 has the smallest specific heat ratio. Compared with the experimental data, the errors of two models are less than 8%.

Table 2 Resonant frequencies of the gas-liquid systems with different working gases

Working gas	Resonant frequency (Hz)		
	LPM	SLPM	Experiment
Ar	6.68	6.63	6.74
N_2	6.13	6.06	6.28
CO_2	6.10	5.84	5.66

4 Conclusions

Based on an acoustic-electric analogy, an LPM and an SLPM are developed to estimate the resonant frequency of a standing-wave thermoacoustic engine with gas-liquid coupling oscillation. The computation with these two models indicates that an addition of the mean working pressure leads to an increase in the resonant frequency, and the resonant frequency decreases with an increase in the gas space volume and with an elongation of the water column. For a resonant tube with fixed dimensions, the water column length dominates the system's behavior; i.e., the resonant frequency still decreases with an elongation of water column, although the elongation of water column results in a decrease in gas space volume. In addition, CO_2 achieves the lowest resonant frequency in the gas-liquid coupling oscillation system, owing to its smallest specific heat ratio compared with Ar and N_2. The comparison of computed results and experimental data shows that both LPM and SLPM can provide a reasonable prediction of the resonant frequency, and in most cases the errors are less than 8%. Compared with LPM, the SLPM without iteration computation is more intuitionistic and more convenient for practical application.

Acknowledgements

The authors would like to thank Prof. Y. MATSUBARA and Prof. A.T.A.M. de WAELE for their meaningful discussion.

References

Backhaus, S., Tward, E., Petach, M., 2004. Travelling-wave thermoacoustic electric generator. *Applied Physics Letters*, **85**(6):1085-1087. [doi:10.1063/1.1781739]

Castrejón-Pita, A.A., Huelsz, G., 2007. Heat-to-electricity thermoacoustic-magnetohydrodynamic conversion. *Applied Physics Letters*, **90**(17):174110. [doi:10.1063/1.2733026]

Chen, G.B., Jiang, J.P., Shi, J.L., Jin, T., Tang, K., Jiang, Y.L., Jiang, N., Huang, Y.H., 2002. Influence of buffer on resonance frequency of thermoacoustic engine. *Cryogenics*, **42**(3-4):223-227. [doi:10.1016/S0011-2275(02)00019-X]

Chen, G.B., Tang, K., Jin, T., 2004. Advances in thermoacoustic engine and its application to pulse tube refrigeration. *Chinese Science Bulletin*, **49**(13):1319-1328. [doi:10.1360/03te0190]

Dai, W., Luo, E.C., Hu, J.Y., Chen, Y.Y., 2005. A novel coupling configuration for thermoacoustically-driven pulse tube coolers: acoustic amplifier. *Chinese Science Bulletin*, **50**(18):2112-2114. [doi:10.1360/982005-482]

Dai, W., Luo, E.C., Yu, G.Y., 2006. A simple method to determine the frequency of engine-included thermoacoustic systems. *Cryogenics*, **46**(11):804-808. [doi:10.1016/j.cryogenics.2006.08.002]

Hu, J.Y., Luo, E.C., Dai, W., Zhou, Y., 2007. A heat-driven thermoacoustic cryocooler capable of reaching below liquid hydrogen temperature. *Chinese Science Bulletin*, **52**(4):574-576. [doi:10.1007/s11434-007-0104-5]

Sugita, H., Matsubara, Y., Kushino, A., Ohnishi, T., Kobayashi, H., Dai, W., 2004. Experimental study on thermally actuated pressure wave generator for space cryocooler. *Cryogenics*, **44**(6-8):431-437. [doi:10.1016/j.cryogenics.2004.02.014]

Swift, G.W., 2002. Thermoacoustics: a Unifying Perspective for some Engines and Refrigerators. Acoustical Society of America Publications, Sewickley, PA, p.98-113.

Tang, K., Chen, G.B., Jin, T., Bao, R., Kong, B., Qiu, L.M., 2005. Influence of resonance tube length on performance of thermoacoustically driven pulse tube refrigerator. *Cryogenics*, **45**(3):185-191. [doi:10.1016/j.cryogenics.2004.10.002]

Tang, K., Bao, R., Chen, G.B., Qiu, Y., Shou, L., Huang, Z.J., Jin, T., 2007. Thermoacoustically driven pulse tube cooler below 60 K. *Cryogenics*, **47**(9-10):526-529. [doi:10. 1016/j.cryogenics.2007.04.003]

Tang, K., Huang, Z.J., Jin, T., Chen, G.B., 2008. Impact of load impedance on the performance of a thermoacoustic system employing acoustic pressure amplifier. *Journal of Zhejiang University-SCIENCE A*, **9**(1):79-87. [doi:10.1631/jzus.A071340]

Tang, K., Lei, T., Jin, T., Lin, X.G., Xu, Z.Z., 2009. A standing-wave thermoacoustic engine with gas-liquid coupling oscillation. *Applied Physics Letters*, **94**(25):254101. [doi:10.1063/1.3157920]

Tu, Q., Li, Q., Wu, F., Guo, F.Z., 2003. Network model approach for calculating oscillating frequency of thermoacoustic prime mover. *Cryogenics*, **43**(6):351-357. [doi:10.1016/S0011-2275(03)00090-0]

West, C.D., 1983. Liquid Piston Stirling Engines. Van Nostrand Reinhold Company, New York, USA, p.1-9.

Yu, G.Y., Luo, E.C., Dai, W., Wu, Z.H., 2007. An energy-focused thermoacoustic-Stirling heat engine reaching a high pressure ratio of 1.40. *Cryogenics*, **47**(2):132-134. [doi:10.1016/j.cryogenics.2006.12.001]